aerospace

MDPI

Article

Investigation of Combustion Performance of Hypergolic Ionic Liquid Fuels Through Injector Design

Vikas Khandu Bhosale *, Keonwoong Lee, Vincent Mario Pierre Ugolini and Hosung Yoon

Research and Development Center, Space Solutions Co., Ltd., 229 Munji ro, Yuseong-gu, Daejeon 34015, Republic of Korea; kwlee@spacesolutions.co.kr (K.L.); vincent@spacesolutions.co.kr (V.M.P.U.); hsyoon@spacesolutions.co.kr (H.Y.)

* Correspondence: vikas@spacesolutions.co.kr

Abstract

Hypergolic ionic liquid fuels are promising alternatives to the toxic hydrazine-based propellants. The present study investigates the combustion performance of a fuel composed of 1-ethyl-3-methylimidazolium thiocyanate ([EMIM][SCN]) and copper(I) thiocyanate (CuSCN) with 95 wt% hydrogen peroxide (H_2O_2) in a 50 N thruster. Two injectors, DM1 (low pressure drop) and DM2 (high pressure drop), were tested at chamber pressures of 10 and 15 bar. The DM1 injector at 15 bar chamber pressure showed high combustion efficiency but suffered from strong pressure oscillations (>10% instability). Switching to the DM2 injector reduced instability (<5%) by increasing the pressure drop. Combustion stability was also improved as the fuel injector orifice diameter/fuel jet velocity (D/V) decreased. FFT analysis showed an instability frequency of 253 Hz with DM1/15 bar, which was higher than the DM1/10 bar test results. In conclusion, the test results revealed the injector or chamber design and pressure drop are the key factors in improving combustion stability for hypergolic propulsion systems.

Keywords: hypergolic fuel; green propellant; combustion instability; ionic liquids; hydrogen peroxide

check for updates

Academic Editor: Stephen D. Heister

Received: 30 May 2025
Revised: 20 August 2025
Accepted: 21 August 2025
Published: 25 August 2025

Citation: Bhosale, V.K.; Lee, K.; Ugolini, V.M.P.; Yoon, H. Investigation of Combustion Performance of Hypergolic Ionic Liquid Fuels Through Injector Design. *Aerospace* **2025**, *12*, 759. https://doi.org/10.3390/aerospace12090759

Copyright: © 2025 by the authors. Licensee MDPI, Basel, Switzerland. This article is an open access article distributed under the terms and conditions of the Creative Commons Attribution (CC BY) license (https://creativecommons.org/licenses/by/4.0/).

1. Introduction

The development of low-toxicity hypergolic propulsion systems is a rapidly growing research area in the propulsion field, driven by the increasing demand for safer and more environmentally sustainable rocket propulsion technologies. Conventional hypergolic propellants, viz., hydrazine and their derivatives, are highly toxic, flammable, and carcinogenic. The permissible exposure limit for hydrazine is 0.01 ppm, significantly below the odor detection threshold (1–3 ppm), making it hazardous even when undetectable by smell (Table 1). Furthermore, the commonly used oxidizer dinitrogen tetroxide (N_2O_4) is also extremely toxic and corrosive. In liquid form, N_2O_4 exists in equilibrium with nitrogen dioxide (NO_2) vapors, which, upon contact with human tissue, especially within the respiratory system, can form nitric or nitrous acid, leading to severe health issues and even death upon prolonged exposure.

In light of these concerns, there has been a significant shift towards the development of green hypergolic propulsion systems. Since then, high-test peroxide (HTP) has emerged as one of the promising monopropellants and oxidizers for bipropellants. It has high density, low vapor pressure, ease of handling, and environmentally benign combustion products [1,2]. Several pioneering studies have reported low-toxicity hypergolic propellants

using HTP, including research from the Naval Air Warfare Center [3], Purdue University [4], Korea Advanced Institute of Science and Technology (KAIST) [5–7], National Institute for Space Research [8], Deutsches Zentrum für Luft- und Raumfahrt (DLR, German Aerospace Center) [9,10], and Lukasiewicz Institute of Aviation [11]. Despite these efforts, no green hypergolic propulsion system has yet reached commercial deployment, and only a few fuel combinations are currently considered viable for future applications.

Table 1. Comparative study of propellants.

	Order Threshold, ppm	**Exposure Limit, ppm**	**Vapor Pressure, Psia at 25 °C**	**Viscosity, cP**
Hydrazine	2–3	0.01	0.96	0.97 at 298 K
MMH	1–3	0.01	3.23	0.855 at 293 K
N_2O_4	1–3	3.0	17.4	0.47 at 293 K

Recent advancements in ionic liquid (IL) technology have introduced new opportunities in green hypergolic propulsion [12–14]. Ionic liquids possess desirable properties such as low vapor pressure, high energy density, and the ability to undergo hypergolic reactions with hydrogen peroxide. Notably, in 2022, DLR conducted the first hot-firing test of a green hypergolic propellant system, HIP_11, which combined 97% H_2O_2 with an ionic liquid fuel comprising 1-ethyl-3-methylimidazolium thiocyanate ([EMIM][SCN]) and 5 wt% copper(I) thiocyanate (CuSCN) [10]. This system achieved steady-state combustion in a 25 N thruster, demonstrating combustion efficiencies exceeding 93%. Additional studies on combustion performance were conducted using various injector configurations (triplet and pentad) and chamber geometries [9]. It was found that a 2-on-1 impinging injector provided more stable combustion, and the elongated combustion chambers (with a characteristic length of 1.2 m) yielded better performance than shorter designs. However, high-frequency pressure oscillations (~1000 Hz) were still observed, posing risks of structural damage. Thus, further evaluations of these propellants across different thruster scales are necessary.

Space Solutions Co., Ltd. (Daejeon, Republic of Korea) has also contributed to the advancement of HTP-based green hypergolic systems. In our recent studies, the combustion characteristics of an ionic liquid fuel, ILethCu01, combined with 95 wt% H_2O_2, were investigated in a 50 N rocket engine [5]. This combination achieved combustion efficiencies exceeding 90% in several cases, although instabilities ranging between 3% and 5% were noted. In this study, experimental campaigns were conducted using different injectors and chambers with another fuel formulation ([EMIM][SCN] + CuSCN). Two type of injectors, DM1 (low pressure drop) and DM2 (high pressure drop), were developed, and tests were conducted at chamber pressures of 10 and 15 bar. The influence of these parameters on combustion efficiency and stability was systematically assessed.

2. Materials and Methods

The ionic liquid [EMIM][SCN] (95%) and copper(I) thiocyanate (CuSCN, 99%) were purchased from Sigma-Aldrich Korea, Seoul. The oxidizer, 95 wt% hydrogen peroxide (H_2O_2), was obtained from HABO, Shanghai, China. The concentration (95.5 ($\pm$2)%) was measured prior to the hot fire test by using a refractometer (PR-59HO, ATAGO Co., Ltd., Tokyo, Japan).

Initially, various concentrations (1–10 wt%) of CuSCN were dissolved in [EMIM][SCN] to prepare fuel blends (Figure 1). Hypergolic drop tests of theses fuels were performed with 95 wt% H_2O_2. The oxidizer (~40 µL) was dropped into the fuel pool (~200 µL). The distance (110 mm) between the oxidizer dispense point and the fuel surface was constant throughout

the experiment. Hypergolic drop tests were then conducted using [EMIM][SCN], both neat and in a solution with CuSCN, with 95 wt% H_2O_2. A high-speed camera (4000 fps, FASTCAM Mini UX-100, Photron, Tokyo, Japan) was used to capture the ignition event. Based on drop test results, the fuel formulation ILCu01 was optimized for further study. Differential scanning calorimetry (DSC) was performed to evaluate thermal properties using a DSC 4000 instrument (PerkinElmer, Shelton, CT, USA) with a nitrogen flow rate of 20 mL/min. Weight loss as a function of temperature was analyzed using a simultaneous DSC-TGA system (STA 6000, PerkinElmer, Shelton, CT, USA) under the nitrogen flow rate of 20 mL/min. Physical properties such as density and viscosity were measured using an Anton Paar viscometer (SVM 3001 Cold Properties, Anton Paar, Graz, Austria). The Newtonian or non-Newtonian behavior of the fuels was measured using ViscoQC 300-L (Anton Paar, Graz, Austria) instrument with spindle type CP-41.

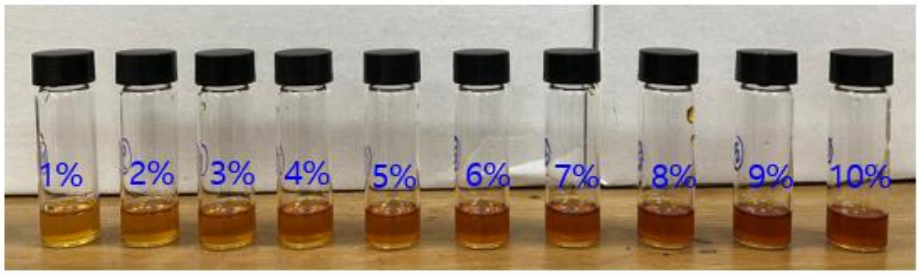


Figure 1. Weight percentages of CuSCN in [EMIM][SCN].

Theoretical performance, such as characteristics velocity, and specific impulse of ILCu01/95 wt% H_2O_2 and MMH/NTO propellants, was simulated using NASA Chemical Equilibrium with Applications (CEA) code. An infinite-area combustion model under frozen flow conditions was applied. The heat of combustion for CuSCN, measured via a bomb calorimeter, was used to determine the heat of formation. The heats of formation of [EMIM][SCN], CuSCN, and H_2O_2 of 52.80 kJ/mol, 308.69 kJ/mol, and −187.79 kJ/mol, respectively, were used for performance calculation (Supporting Information SI-7). These calculations were performed at a constant chamber pressure of 10 bar and nozzle expansion ratio of 100, across a range of oxidizer-to-fuel (O/F) ratios.

The static fire test bed setup is described in a previous study [5], and a schematic is provided in Supporting Information SI-2. The engine (injectors and chambers) was designed based on theoretical calculations, targeting chamber pressures of 10 and 15 bar and a vacuum thrust of 50 N at area ratio of 2.52 for 10 bar, and 3.79 for 15 bar (Figure 2). Moreover, the injector and chamber images are given in Supporting Information SI-6. Single-element, unlike triplet (O-F-O) injectors were developed: Development Model 1 (DM1) and Development Model 2 (DM2). The impinging angle was fixed at 90° with standard deviation 1°. The DM1 injector was designed with a pressure drop equal to 20% of the chamber pressure, as a baseline for liquid thruster ignition [15,16].

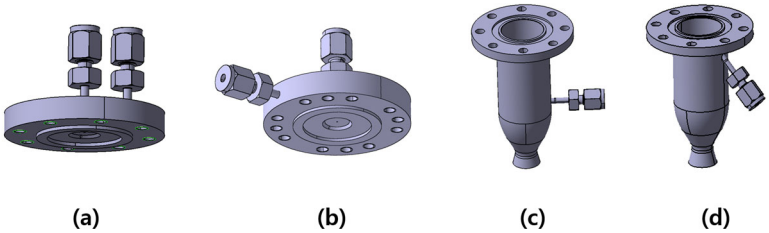


Figure 2. The 3D representation of (**a**) DM1 injector, (**b**) DM2 injector, (**c**) 10 bar chamber, and (**d**) 15 bar chamber.

Based on the hot-fire test results, the DM2 injector was developed with a higher pressure drop of 40–50% of the chamber pressure. The detailed specifications of the DM1 and DM2 injectors and chambers are given in the Supporting Information SI-1. The mass flow rate of the fuel and oxidizer was measured using the differential pressure transducer (±0.25% FSO). The ETM (Engineering Treatment Model) pressure transducer with accuracy of ±0.5% (FSO) was used to measure the pressure data. All pressures were measured as absolute (bar). Static fire tests were performed with a maximum duration of 2 s, across different O/F ratios. Key performance parameters such as experimental characteristic velocity, combustion efficiency, and combustion instability were calculated using experimental data, with equations reported elsewhere [5]. Fast Fourier Transform (FFT) analysis was performed using Matlab wavelet function. The combined standard uncertainty of measured quantities was calculated by using Equation (1), which is described in [9].

$$u_f^2 = \sum_{i=1}^{n} \left(\frac{\partial f}{\partial x_i} \right)^2 u^2 \left(x_i \right) \quad (1)$$

where u_f is the combined standard uncertainty as function of f, $u(x_i)$ is the standard uncertainty in the input variable x_i, and $\left(\frac{\partial f}{\partial x_i} \right)$ is the sensitivity coefficient.

3. Results and Discussion

3.1. Hypergolic Drop Test

The measurement of hypergolic fuel ignition properties in terms of ignition delay time (IDT) has significance in choosing a fuel candidate for propellant application. Ignition delay time was measured by calculating time difference between the fuel with oxidizer contact and the first visible flame seen. An oxidizer dropper and a fuel pool were employed and the distance between the drop point of the oxidizer and the fuel pool surface was kept constant throughout the experiment. [EMIM][SCN] exhibited an IDT of 24 ms with 95 wt% H_2O_2. Further, 1–10 wt% CuSCN in [EMIM][SCN] were dissolved and tested with 95 wt% H_2O_2, the IDT was lowered to 14 ms for 5 wt% CuSCN, as shown in Figure 3. Further increases in additive concentration did not improve the IDT. Similar results were also reported by DLR [10,17]. The fuel combination 5 wt% Cu in [EMIM][SCN] is named hereafter as 'ILCu01'. Figure 4 shows the high-speed camera images with the lowest IDT of [EMIM][SCN] and ILCu01 fuel. As the CuSCN concentration increased in the [EMIM][SCN], ignition of fuel with 95 wt% H_2O_2 revealed an intense ignition behavior [17].

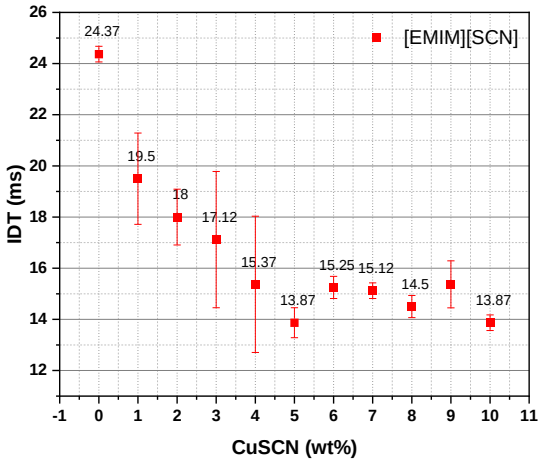
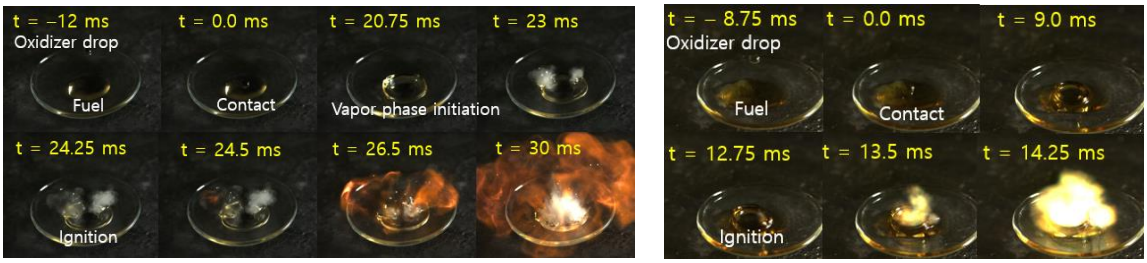


Figure 3. Ignition delay time of fuel with different concentrations of additive with 95 wt% H_2O_2 (fuel: [EMIM][SCN]; additive: CuSCN).

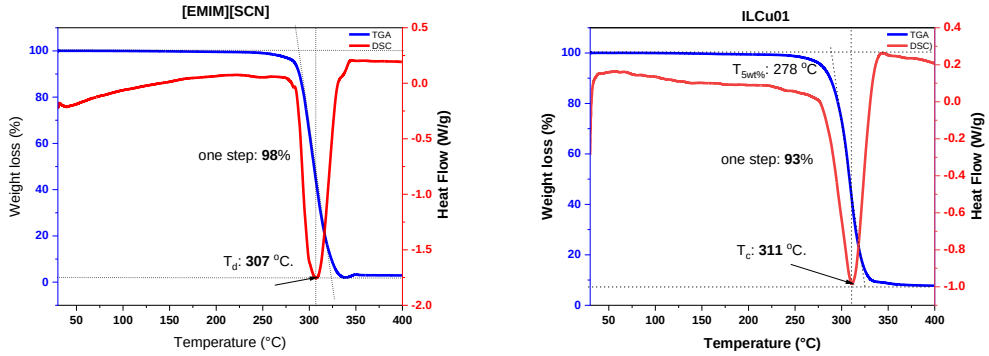


(**a**) (**b**)

Figure 4. High speed camera images of (**a**) [EMIM][SCN] with 95 wt% H_2O_2 and (**b**) ILCu01 with 95 wt% H_2O_2.

3.2. Physicochemcial Properties of Fuel

Ionic liquids are viscous materials compared to hydrazine-based fuels [9]. The viscosity of [EMIM][SCN] was 22 mPa·s. However, the addition of an additive to an ionic liquid makes it more viscous; hence, ILCu01 revealed a viscosity of 32 mPa·s. Another significant property of fuel is density, which was (ILCu01: 1.11 g/cm^3) higher than MMH (0.78) fuel. High density values can help to improve the density-specific impulse of a propellant. Moreover, ILCu01 exhibited a wide liquid range from −80 °C to 278 °C (temperature at 5 wt% weight loss), which demonstrates the working ability of the fuel at different temperatures (Figures 5 and 6). A negative DSC peak was observed during the thermal decomposition of the fuel in a nitrogen atmosphere, indicating an endothermic process. Furthermore, it was observed that the thermal stability of ILCu01 was improved by 4 °C compared to the [EMIM][SCN] fuel. This may be due to intermolecular interactions between CuSCN and [EMIM][SCN], and similar results were also reported by Lauck et al. [17].



(**a**) (**b**)

Figure 5. Thermal analysis of fuels: (**a**) simultaneous DSC-TGA analysis of [EMIM][SCN]; (**b**) simultaneous DSC-TGA analysis of ILCu01.

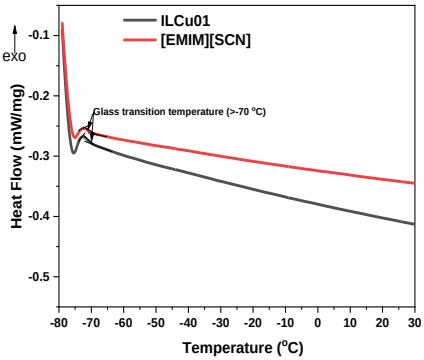


Figure 6. Low-temperature DSC of [EMIM][SCN] and ILCu01.

3.3. Theoretical Performance

The rocket performance, such as characteristic velocity and specific impulse, is a significant factor for measuring the efficiency of a propellant. In chemical propulsion, the performance is in the order of cryogenic propellant > liquid propellant > solid propellant. The NASA chemical equilibrium calculation (CEA) can be used to find the best performing chemicals before testing in a real rocket engine [18,19]. Based on the theoretical results, it was easy to select the fuel for further study. The performance parameters were used to design a rocket engine under vacuum condition. The specific impulse and characteristic velocity of ILCu01/95 wt% H_2O_2 were increased then decreased with increasing O/F ratios (Figure 7). A concave downward curve was observed with optimum performance of C* of 1547 m/s at O/F 3.6. However, the optimum Isp of 305 s was observed at O/F of 3.8. MMH/NTO gives the maximum C* and Isp values of 1704 m/s and 325 s, respectively, under similar conditions, which were higher than those of ILCu01/95 wt% H_2O_2. Interestingly, the density-specific impulse of ILCu01/95 wt% H_2O_2 was 409 g.s/cm^3, which was 7.34% higher than that of MMH/NTO (379 g.s/cm^3). The maximum C* and Isp performance were observed at different O/F ratios, because C* was independent of nozzle dimensions. The adiabatic temperature of ILCu01/95 wt% H_2O_2 was 2775 K, which was lower than that of the MMH/NTO (3084 K) propellant.

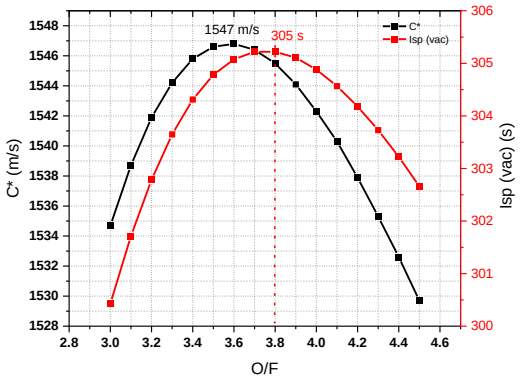


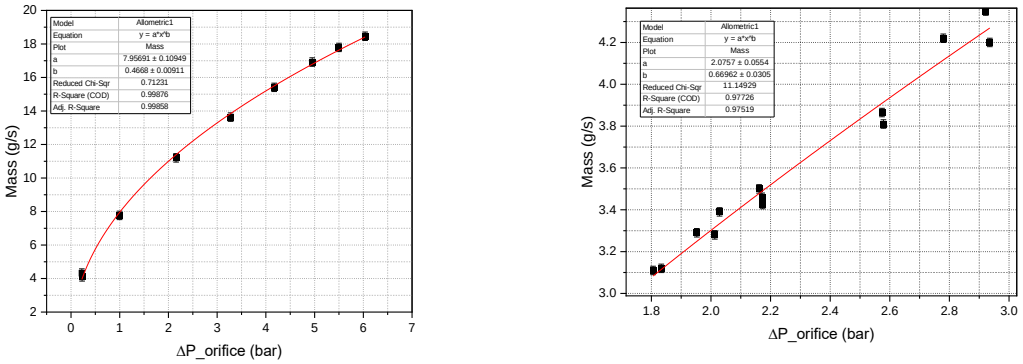
Figure 7. Theoretical analysis of ILCu01/95 wt% H_2O_2 propellant using NASA CEA code.

3.4. Hot Fire Test Results

3.4.1. Mass Flow Rate Calibration

Prior to conducting the firing test, the calibration of the mass flow rate is a critical step. Several methods are available for measuring the mass flow rate. In this study, a differential pressure transducer was used to measure the mass flow rate based on the pressure drop across an orifice plate installed in the line. The metering valve was adjusted to vary the mass flow rate while maintaining a constant inlet pressure. The differential pressure was recorded, corresponding to changes in mass flow rate. Multiple measurements were taken for the fuel and oxidizer at different pressure drops, and the results are presented in Figure 8.

As shown in Figure 8a, the oxidizer mass flow rate vs. pressure drop (ΔP) shows an allotropic fitting curve. Since hydrogen peroxide behaves as a Newtonian fluid with a Reynolds number greater than 1000, the curve fitting was accurate. In Figure 8b, the fuel mass measurements showed a scattered trend, even for fluids that show a Newtonian nature (Supporting Information Figure S4), of mass flow rate vs. pressure drop (ΔP) along with the fitting line. This may be due to the low Reynolds number below 1000, where the discharge coefficient was not constant during measurement [20]. Furthermore, an allotropic curve was fitted to measure the mass flow rate of the fuel.



(**a**) (**b**)

Figure 8. Mass flow rate calibration (**a**) 95 wt% H_2O_2 oxidizer; (**b**) fuel.

Three different tests were conducted by considering the injector model/chamber pressure/fuel such as DM1/10 bar/ILCu01, DM1/15 bar/ILCu01, and DM2/10 bar/ILCu01. The stoichiometric O/F ratio of this propellant was 4.4 with control precision of ±1.05% with different O/F values (Figure 9). As the fuel and oxidizer were controlled by the metering valve, keeping a constant chamber tank pressure, it was difficult to adjust the exact mass flow rate at a stoichiometric ratio.

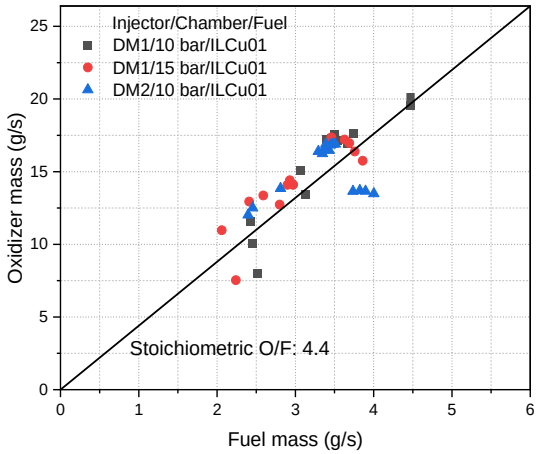


Figure 9. Propellant mass flow rate and oxidizer-to-fuel ratio.

3.4.2. Thruster Behavior During Firing Test

Initially, the firing tests were conducted using the DM1 injector at two different chamber pressures, 10 bar and 15 bar, and a further DM2 injector was used with a 10 bar chamber (Supporting Information SI-3). A total of three tests series were conducted by using the ILCu01/95 wt% H_2O_2 propellant. The propellant composition was different from that studied by Lauck et al. for a 22 N thruster [10]. A representative case with a similar O/F ratios for DM1 at 10 bar and 15 bar was selected for comparison (Figure 10). In both tests, the oxidizer and fuel mass flow rates were set at ~17 g/s and ~3.7 g/s, respectively, resulting in an O/F ratio of 4.6 and a relatively high total mass flow rate.

The pressure drops for Test 11 (DM1/10 bar) were 1.79 bar and 1.81 bar for the fuel and oxidizer injectors, respectively. A similar pressure drop was also observed in the DM1/15 bar chamber test (Test 12, Supporting Information Table S4). Figure 10a,b clearly illustrate the differences in chamber pressure oscillations. More pronounced oscillations are exhibited at the 15 bar chamber; however, the characteristic velocity and combustion efficiency improve by approximately 147 m/s and a corresponding 9%, respectively, when

compared to the 10 bar chamber (Test 10, DM1/10 bar). A similar combustion instability was also reported by Sarritzu et al. [9] during their study in a large chamber.

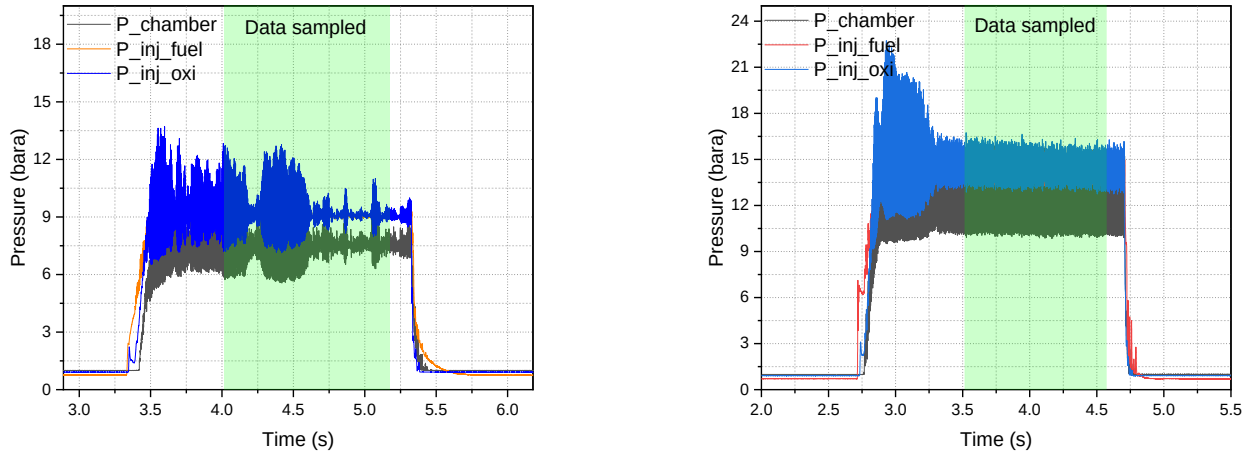


Figure 10. Hypergolic combustion in (**a**) DM1 injector 10 bar chamber (Test 10) and (**b**) DM1 injector 15 bar chamber (Test 12).

Despite these improvements, combustion instability was higher for the 15 bar chamber experiment. Combustion instability values for DM1/10 bar (Test 10) and DM1/15 bar (Test 12) were 9.4% and 13.4%, respectively. A Fast Fourier Transform (FFT) analysis was conducted to compare the instability intensities and peak frequencies across the tests. Previous studies [21] have shown that modifications in propellant properties or thruster geometry, particularly the characteristic length, can reduce instabilities. The frequency amplitude graph clearly shows differences in instability amplitudes between the 10 bar and 15 bar chambers for the DM1 injector (Figure 11). A high-intensity low-frequency instability was observed in the 15 bar chamber compared to the 10 bar chamber. The peak frequency recorded by the FFT for the DM1/15 bar test was 253 Hz, with an amplitude of 0.75 bar. In contrast, for the DM1/10 bar test, the peak frequency was 222 Hz with an amplitude of 0.27 bar. These results clearly demonstrate that combustion chamber pressure significantly influences combustion instability, similarly to the DLR study [9]. This low-frequency combustion instability occurs due to the coupling between the feed system and the combustion chamber, a phenomenon known as chugging [16,22]. SST time–frequency studies also reveal the instability over time (Supporting Information Figure S2). Further testing is necessary to analyze instability behavior across a broader range of chamber pressures. It was assessed that the low injector pressure drop may have contributed to the observed instabilities. Therefore, to improve stability, a new injector model, DM2, was developed, targeting a pressure drop of 40–50% of the chamber pressure.

The performance of the DM1 and DM2 injectors was compared at a chamber pressure of 10 bar (Figure 12). For consistency, the oxidizer mass flow rate was maintained at 17 g/s, and the fuel mass flow rate was adjusted to 3.5 g/s, resulting in an O/F ratio of 4.8 for both tests. The pressure drops from the oxidizer and fuel injectors for the DM2 injector (Test 12) were 5.2 bar and 4.0 bar, respectively. This higher pressure drop may have contributed to the reduced instability observed with the DM2 injector compared to DM1.

In comparison with DM1, the combustion instability for DM2 was notably lower, below 5% (Supporting Information Table S5). The FFT analysis for the DM2/10 bar test did not yield a clear instability frequency, likely due to the lower data sampling rate of 1000 Hz, whereas the DM1 tests were conducted at 10,000 Hz. Consequently, while instabilities were

still observed in Test 12 (Supporting Information Figure S3a), particularly around a peak frequency of 220 Hz, these results require confirmation through higher-resolution testing.

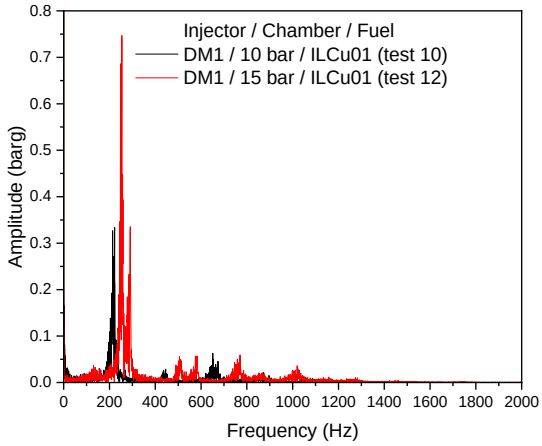
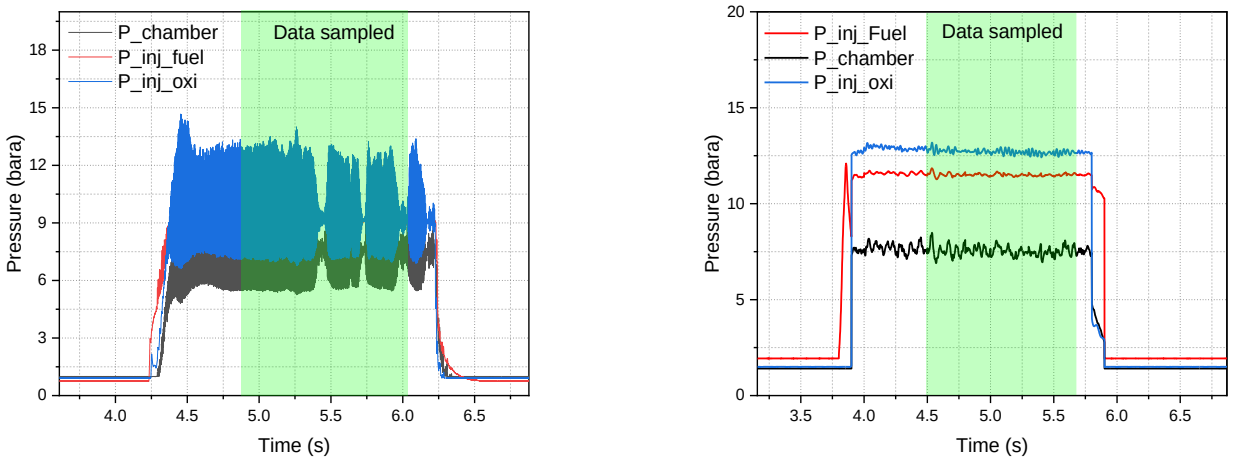


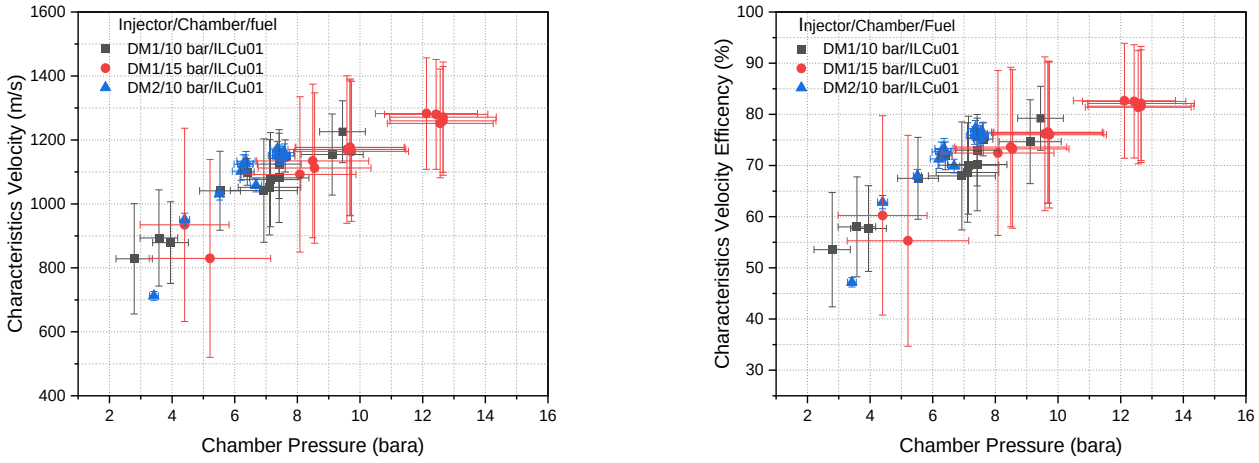
Figure 11. Excitation frequency of the DM1 injector with 10 and 15 bar chambers.



(**a**) (**b**)

Figure 12. Hypergolic combustion test of (**a**) DM1 injector 10 bar chamber (Test 9); (**b**) DM2 injector 10 bar chamber (Test 12).

Based on the combustion data, experimental characteristic velocities from the DM1 and DM2 injector tests were calculated (Figure 13a), and combustion efficiency was estimated by comparing with the ideal characteristic velocity (Figure 13b). Figure 13a,b reveals that the characteristics velocity (C*) and characteristic velocity efficiency (ηC*) were improved with the increase in chamber pressure. The standard uncertainties for the DM1 injector with 10 and 15 bar chambers were higher than for DM2/10 bar. This is attributed to the higher pressure fluctuations associated with the DM1 injector test results, which resulted in greater standard uncertainty in chamber pressure. Combustion efficiency and standard uncertainty were highest for the DM1/15 bar test. For example, the DM1/10 bar (Test 12) showed a characteristic velocity of 1226 m/s, whereas DM1/15 bar (Test 11) achieved 1280 m/s at a similar O/F ratios. Accordingly, the combustion efficiency for the 10 bar test was 79%, compared to 83% for the 15 bar test for DM1. Moreover, the combustion instability was significantly lower for DM2/10 bar (below 5%) compared to DM1, which showed instabilities exceeding 5% for both the 10 and 15 bar tests. These findings suggest that injector pressure drop plays a critical role in the steady operation of a thruster.



(**a**) (**b**)

Figure 13. Characteristic velocity (**a**) and characteristic velocity efficiency (**b**) vs. chamber pressure of each test.

Furthermore, the relationship between the fuel orifice diameter to velocity ratio (D/V)fuel) and combustion instability was investigated (Figure 14). The results indicated that combustion instability decreased as (D/V)fuel decreased. Using the DM2 injector, it was observed that when (D/V)fuel dropped below 0.05, stable combustion was achieved. Thus, estimating (D/V)fuel during the thruster design phase may allow for optimization of thruster performance while minimizing instabilities.

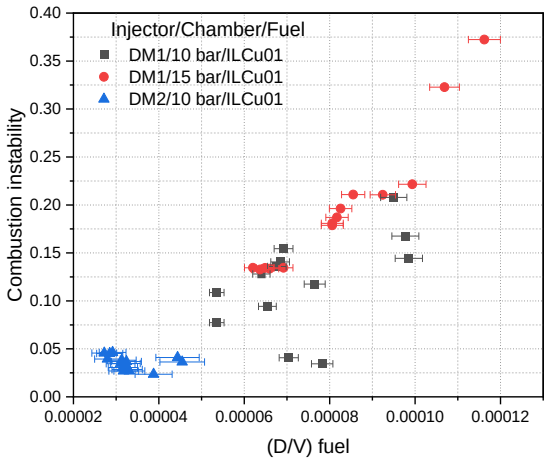


Figure 14. D/V and combustion instability relation.

4. Conclusions

In this study, the influence of injector design was evaluated for a thruster using hydrogen peroxide and a hypergolic fuel. The ignition delay time (IDT) and thermal properties of ILCu01 were reproduced to confirm the performance and thermal stability, and the results were compared with studies from DLR. Furthermore, ILCu01 was tested with 95% H_2O_2 in a 50 N thruster to investigate combustion behavior under different injector designs. The DM1 injector design was initially considered with a 10–20% injector pressure drop relative to the chamber pressure. However, it was found that this pressure drop was not sufficient to sustain steady-state combustion, despite yielding better combustion efficiency. In contrast, the DM2 injector design, which employed a 40–50% pressure drop, showed improved combustion stability. Additionally, the ratio between the injector

diameter and fuel injection velocity appears to determine a critical threshold (~0.05 m/s), beyond which combustion instability occurs. Further experiments are recommended to verify whether these design parameters are applicable to other types of propellants.

Supplementary Materials: The following supporting information can be downloaded at https://www.mdpi.com/article/10.3390/aerospace12090759/s1. References [23–25] are cited in the supplementary materials. Specification of injectors and chambers, Schematic of hypergolic propellant test bed (P&ID), Hot fire test results, FFT results, Fluid properties of ILCu01, Injectors and chambers images, Heat of formation of CuSCN.

Author Contributions: Conceptualization, V.K.B.; methodology, V.K.B.; investigation, V.K.B.; formal analysis, V.K.B., K.L. and V.M.P.U.; validation, V.K.B., K.L. and V.M.P.U.; visualization, V.K.B. and K.L.; supervision, V.K.B.; project administration, V.K.B.; writing—original draft, V.K.B. and V.M.P.U.; writing—review and editing, V.K.B.; resources, H.Y. All authors have read and agreed to the published version of the manuscript.

Funding: This research received no external funding.

Data Availability Statement: Data are contained within the article.

Conflicts of Interest: Author Vikas Khandu Bhosale was employed by the company Space Solutions Co., Ltd. The remaining authors declare that the research was conducted in the absence of any commercial or financial relationships that could be construed as a potential conflict of interest.

Abbreviations

The following abbreviations are used in this manuscript:

IL	Ionic liquid
[EMIM][SCN]	1-ethyl-3-methyl imidazolium thiocyanate
IDT	Ignition Delay Time
FFT	Fast Fourier Transform
DLR	Deutsches Zentrum für Luft- und Raumfahrt
WSST	Wavelet Synchrosqueezed Transform
DM1/10 bar	Development Model 1 Injector (DM1)/Designed chamber pressure (10 bar)
DM1/15 bar	Development Model 1 Injector (DM1)/Designed chamber pressure (15 bar)
DM2/10 bar	Development Model 2 Injector (DM2)/Designed chamber pressure (10 bar)
MMH	Monomethyl Hydrazine
NTO	Nitrogen Tetroxide
DSC-TGA	Differential Scanning Calorimetry- Thermogravimetric Analysis
HTP	High-Test Peroxide
SST	Synchrosqueezing Transform
NASA	National Aeronautics and Space Administration
D/V	Diameter/Velocity

References

1. Rarata, G.; Florczuk, W. Novel Liquid Compounds As Hypergolic Propellants With HTP. *J. KONES Powertrain Transp.* **2016**, *23*, 271–278. [CrossRef]
2. Clark, J. *IGNITION! An Informal Histroy of Liquid Propellants*; Rutgers University Press: New Brunswick, NJ, USA, 1972; ISBN 0813507251.
3. Rusek, J.J.; Minthorn, M.K.; Purcell, N.L.; Pavia, T.C.; Grote, J.R.; Hudson, G.C.; Mckinney, B. *Non-Toxic Homogeneous Fuel (NHMF) Development for Hypergolic Bipropellant Engines*; Naval Air Warfare Center Weapons Division China Lake: Lake, CA, USA, 1996.
4. Austin, B.L.; Heister, S.D. Characterization of Pintle Engine Performance for Nontoxic Hypergolic Bipropellants. In Proceedings of the 38th AIAA/ASME/SAE/ASEE Joint Propulsion Conference & Exhibit, Indianapolis, Indiana, 7–10 July 2002. [CrossRef]
5. Bhosale, V.K.; Lee, K.; Yoon, H.; Kwon, S. Green Bipropellant: Performance Evaluation of Hypergolic Ionic Liquid-Biofuel with Hydrogen Peroxide. *Fuel* **2024**, *376*, 132688. [CrossRef]

6. Kang, H.; Jang, D.; Kwon, S. Demonstration of 500 N Scale Bipropellant Thruster Using Non-Toxic Hypergolic Fuel and Hydrogen Peroxide. *Aerosp. Sci. Technol.* **2016**, *49*, 209–214. [CrossRef]
7. Kang, H.; Lee, E.; Kwon, S. Suppression of Hard Start for Nontoxic Hypergolic Thruster Using H_2O_2 Oxidizer. *J. Propuls. Power* **2017**, *33*, 1111–1117. [CrossRef]
8. Maschio, L.J.; de Araújo, E.P.; Pereira, L.G.F.; Gouvêa, L.H.; Vieira, R. Assessing the Performance of a Green Liquid Fuel Hypergolic with Hydrogen Peroxide in a 50 n Bipropellant Thruster. *Int. J. Energ. Mater. Chem. Propuls.* **2021**, *20*, 21–30. [CrossRef]
9. Sarritzu, A.; Pasini, A.; Merz, F.; Werling, L.; Lauck, F. Experimental Investigation of Combustion Performance of a Green Hypergolic Bipropellant Based on Hydrogen Peroxide. *Acta Astronaut.* **2024**, *219*, 278–290. [CrossRef]
10. Negri, M.; Lauck, F. Hot Firing Tests of a Novel Green Hypergolic Propellant in a Thruster. *J. Propuls. Power* **2022**, *38*, 467–477. [CrossRef]
11. Lukasiewicz—Institute of Aviation. New Green Hypergolic Propellant—Potential Gamechnager for in-Space Propulsion. 2023. Available online: https://ilot.lukasiewicz.gov.pl/en/green-hypergolic-propellant/ (accessed on 22 May 2025).
12. Seo, M.; Bhosale, V.K.; Im, H.; Kwon, S. Performance Improvement of Triglyme-Based Fuels Using an Ionic Liquid with Hydrogen Peroxide. *Combust. Flame* **2024**, *270*, 113719. [CrossRef]
13. Bhosale, V.K.; Gwak, J.; Kim, K.S.; Churchill, D.G.; Lee, Y.; Kwon, S. Rapid Ignition of "Green" Bipropellants Enlisting Hypergolic Copper (II) Promoter-in-Fuel. *Fuel* **2021**, *297*, 120734. [CrossRef]
14. Bhosale, V.K.; Kulkarni, P.S. Ultrafast Igniting, Imidazolium Based Hypergolic Ionic Liquids with Enhanced Hydrophobicity. *New J. Chem.* **2017**, *41*, 1250–1258. [CrossRef]
15. Huang, D.H.; Huzel, D.K. *Modern Engineering for Design of Liquid-Propellant Rocket Engines*; American Institute of Aeronautics and Astronautics: Washington, DC, USA, 1992; ISBN 1563470136.
16. Suttan, G.P.; Biblarz, O. *Rocket Propulsion Elements*, 7th ed.; Suttan, G.P., Biblarz, O., Eds.; John Wiley & Sons, Inc.: New York, NY, USA, 2001; ISBN 0471326429.
17. Lauck, F.; Balkenhohl, J.; Negri, M.; Freudenmann, D.; Schlechtriem, S. Green Bipropellant Development—A Study on the Hypergolicity of Imidazole Thiocyanate Ionic Liquids with Hydrogen Peroxide in an Automated Drop Test Setup. *Combust. Flame* **2021**, *226*, 87–97. [CrossRef]
18. Mcbride, B.J.; Gordon, S. Computer Program for Calculation of Complex Chemical Equilibrium Composition and Applications II. User Manual and Pogram Description. In *NASA Reference Publication 1311*; NASA Lewis Research Center: Cleveland, OH, USA, 1996.
19. Gordon, S.; McBride, B.J. *Computer Program for Calculation Complex Chemical Equilibrium Compositions and Applications, I. Analysis*; NASA Lewis Research Center: Cleveland, OH, USA, 1994; ISBN 1995001376.
20. Lefebvre, A.H.; McDonell, V.G. *Atomization and Sprays*; Taylor & Francis Group; CRC Press: Boca Raton, FL, USA, 2017; ISBN 9781498736251.
21. Kyu-seop, K. Ignition and Reactive Spray Characteristics of High Test Peroxide-Based Rapid Hypergol. PhD Thesis, Korea Advanced Institute of Science and Technology, Daejeon, Republic of Korea, 2022.
22. Huzel, D.K.; Huang, D.H. *Design of Liquid-Propellant Rocket Engines*; NASA: Washington, DC, USA, 1967.
23. Chase, M.W., Jr. *NIST-JANAF Thermochemical Tables*, 4th ed.; American Institute of Physics: College Park, MD, USA, 1998; pp. 1–1951.
24. Available online: https://en.wikipedia.org/wiki/Hydrogen_peroxide (accessed on 22 May 2025).
25. Zaitsau, D.H.; Emel'yanenko, V.N.; Verevkin, S.P.; Heintz, A. Sulfur-Containing Ionic Liquids. Rotating-Bomb Combustion Calorimetry and First-Principles Calculations for 1-Ethyl-3-methylimidazolium Thiocyanate. *J. Chem. Eng. Data* **2010**, *55*, 5896–5899. [CrossRef]

Disclaimer/Publisher's Note: The statements, opinions and data contained in all publications are solely those of the individual author(s) and contributor(s) and not of MDPI and/or the editor(s). MDPI and/or the editor(s) disclaim responsibility for any injury to people or property resulting from any ideas, methods, instructions or products referred to in the content.